35th Annual International Conference of the IEEE EMBS
Osaka, Japan, 3 - 7 July, 2013

Preparation of Decellularized Meniscal Scaffolds using Sonication Treatment for Tissue Engineering

A. Azhim, T. Ono, Y. Fukui, Y. Morimoto, K. Furukawa, T. Ushida

Abstract—**Scaffolds play a key role in the process of regeneration and morphogenesis of tissue or organ. We have developed a novel sonication decellularization system to prepare decellularized bio-scaffolds in a short treatment time. The aim of the study is to investigate sonication decellularization condition that completely decellularize meniscus can be changed as well as to maintain the biomechanical parameters of scaffolds. The meniscus samples were decellularized using sonication treatment. The treated samples were evaluated histologically by EVG for cell removal, picrosirius red for content of collagen type I and III, and safranin-O/fast green staining for content of glycosaminoglycan, and SEM for observation of scaffold surface. Indentation apparatus was used to analyze the unconfined deformation under load of native and decellularized menisci. The load parameters which are stiffness, compression and residual force were not significantly different compare with native and sonicated scaffolds. However, the content of extracellular matrix and its fiber alignment changed significantly due to sonication treatment as observed by SEM and safranin-O/fast green staining, respectively. The removal of immunogenic cell components by sonication decellularization as well as maintain its biomechanical strength of decellularized scaffolds, so that it has potential to use as an implant material for tissue engineering of menisci.**

I. Introduction

The menisci are paired fibro-cartilaginous structures vital to the maintenance of knee health. Each meniscus transmits greater than 50% of load across its compartment, absorbs shock, and facilitates synovial fluid distribution [1]. In older patients, a meniscus tear may not be of traumatic origin but rather part of degenerative changes in the knee. Various tear patterns and configurations have been described. These includes: radial tears, peripheral and longitudinal tears, bucket-handle tears, horizontal cleavage tears, and complex and degenerative tears. These tears can then further classified by their proximity to meniscus blood supply, namely whether they are located in the "red-red," "red-white," or "white-white" zones. Tears occurred in red-white or white-white zones have less predictable success to repair. As other alternative, replacement of the meniscus using allograft was reported to have significant result with the survival rate ranging from 50% to 82% [2]. Major reasons are biomechanical failure, cell toxicity and immunological response of the host towards scaffolds or towards its degradation of products [3]. Tissue engineering holds the potential of a new approach to the repairing and reconstruction of tissue and organs damaged by disease and accident. The essential part of tissue engineering include biochemical factors, mechanical stimulation and scaffolds. A three-dimensional (3D) scaffold provides an extracellular matrix (ECM) analog which functions as a necessary template for host infiltration and a physical support to guide the differentiation and proliferation of cells into the targeted functional tissue or organ [4]. In the tissue engineering approach, bio-artificial scaffolds were generally prepared using decellularization process [5]. The decellularization process can be achieved by using some approaches. Since, conventional methods take an extended period to decellularize cartilage tissues, e.g. menisci. There is a problem of denaturing them [6].

In our study, we have attempted to remove cells from its ECM with an assisted-ultrasonic energy on the decellularization treatment. To engineer scaffolds for tissue/organ transplantation, a complete decellularization is required to decrease the immune rejection. The aim of the present study is to investigate sonication decellularization condition that completely decellularize meniscus can be changed as well as to maintain the biomechanical parameters of scaffolds.

II. METHODS

A. Sonication Decellularization System

A decellularization system has developed using sonication treatment as shown in Fig. 1.

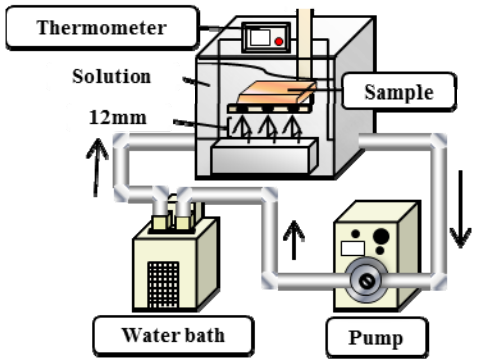

Fig. 1 Sonication decellularization system consists of ultrasonic device, pump, cooling water bath, reactor and temperature

The decellularization system consists of a commercially

A. Azhim is with Malaysia-Japan International Institute of Technology, University of Technology Malaysia, 54100 Kuala Lumpur Malaysia. Tel: 60-3-2203-1295, fax: 60-3-2203-1266, Email: azhim@ic.utm.my; and visiting researcher of Tokyo Denki University, Japan

T. Ono, Y. Fukui are with Division of Life Science and Engineering, Department of Science and Engineering, Tokyo Denki University, Hatoyama, Japan.

Y. Morimoto is with Dept. of Int. Physiol. Bio-Nano Medicine, National Defense Medical College, Tokorozawa, Japan.

K. Furukawa is with Dept. of Mechanical Engineering, The University of Tokyo, Hongo, Japan.

T. Ushida is with The Center for Disease Biology and Integrative Medicine, Faculty of Medicine, The University of Tokyo, Hongo, Japan

available ultrasonic device (Fx-500-35/72/110/170K, Flexonic), a roller pump (RP-1000, Eyela), a constant temperature water bath (LTB-250, As-One), a temperature monitor (TR-71U, T&D) and a custom-made reactor. Due to increase of solution temperature by sonication, we set a sensor beside the sample in the reactor to control temperature at constant. The experiments were performed at a constant temperature of 35±1°C [7]. The bovine meniscus was obtained from a local slaughterhouse (Tokyo Shibaura Organ Co. Ltd, Japan). The samples were cut into approximately 10 mm width and 3 mm thick from the surface to prepare 10 mm ×10 mm×5 mm sample before being used for treatment and indentation testing. The samples were sonicated in the middle part from the surface. We fixed the samples in reactor at depth of approximately 12 mm from the irradiated ultrasonic device. We sonicated the samples at a constant circulating of 0.1% (w/v) sodium deoxycholate sulfate SDS detergent solution for 10 hours. We set frequency of ultrasound to 40 kHz. For control, a typical immersion treatment was performed in static state using the similar detergent solution and temperature. After decellularization treatment, the samples were immersed in PBS and subsequently in DMEM for four days and one day, respectively.

B. Histology

Histological analysis was performed to evaluate tissue integrity and cell removal. We sectioned decellularized samples following standard protocols. We fixed the samples with 4% paraformaldehyde (PFA) for 24 hours at 4°C. We mounted it on Surgipath (FSC22, Leica, USA) and frozen it in dry ice. We cut the samples with a cryostat (CM1510S, Leica, USA) into 8-um frozen sections and stained them with elastic van Gieson (EVG) (Fig. 4), picrosirius red (Fig. 5), safranin-O and fast green (Fig.6). The samples were dehydrated with sequential ethyl alcohol gradient (50, 60, 70, 80, 90 and 100%×2 for 5 minutes each gradient) and xylene (2×5 minutes). The staining of EVG, picrosirius red and safranin-O/fast green is performed to analyzed the cell removal, collagens and glycosaminoglycan (GAG) contents (n= 3), respectively. The images were analyzed with Image J software (National Institutes of Health, US).

C. Scanning Electron Microscopy

We fixed the treated tissue with PFA for 24 hours at room temperature. We dehydrated the samples with a series of ethanol solutions of increasing concentration, beginning with 50% and progressing through 60%, 70%, 80%, 90% and 100% for 20 minutes each. We transferred to t-butyl alcohol (TBA) in 30 min at 4°C. We freeze-dried the sample for approximately 3 hours with a freeze drying device (JFD-310, JEOL). We sputter coated sample with gold (Au) for 60s using a Fine Coater (JFC-1200, JEOL) [15]. We then visualized surface of samples using a scanning electron microscope (JSM-5310LVB, JEOL) as shown in Fig. 7. The Area of channels was analyzed from diameter with Image J software.

D. Biomechanical testing

Six samples used for biomechanical testing were performed

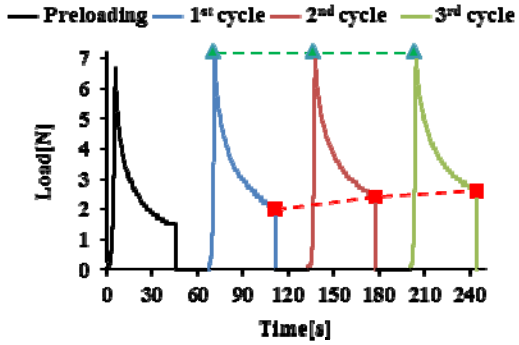

Fig. 2 Load curve of test cycle consist of four repetitive cycles shows the graphical course of preload, dynamic and static compression and relaxation. Note that the linear-elastic slope is obtained during dynamic compression.

for each three time of measurement. Three squares with 6 mm on a side and depth of 3.0 mm were cut out of the middle portions perpendicular to the horizontal plane. The surface of the menisci was oriented perpendicular to the indentation testing device. These squares were put into a custom made device and the upper part of the cylinder was shaped to create a surface parallel to the base. The meniscus samples were then tested by a repetitive ball indentation test, as described previously. The test was performed as a minimally constraint compression–relaxation test with a universal testing machine (MX-5000N, IMADA) and a 3 mm steel ball at the tip of the indenter. The testing machine was used with a digital force analyzer (FA PLUS, IMADA). The meniscus samples were kept moist throughout the experiments using physiologic saline solution. Indenter position zero was at the level of the base of the cavity. As in Fig. 2 and Fig. 3, it is necessary to indent the sample at preloading and measure from 1st cycle loading to provide a stable peak value at maximum loading. The indentation testing consists of three phases: dynamic compression with a constant load velocity of 10 mm/min until 7 N; static compression of the sample for 40 s with a load of 7 N; relaxation of the sample with a constant unload velocity of 10 mm/min until a load of 0 N. After an interval of 30 s, the new test cycle started until a total number of four test cycles were reached and obtained the force-time (F-T) graph as shown in Fig. 2. By changing the display mode, force-displacement (F-D) graph was obtained as shown in Fig. 3. Measurements are performed repetitively 5 times for each sample. Load, indenter position, and time were displayed by a recorder software (F-S Recorder, IMADA) and three values could be calculated: (1) Stiffness determined from the linear elastic slope of the loading curve between 2 and 5 N as shown

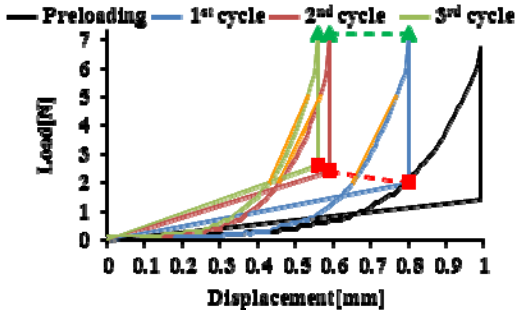

Fig. 3 The Load-displacement graph

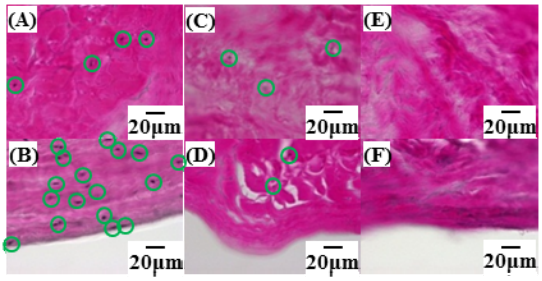

Fig. 4 Photograph of EVG staining of native (A, B), immersion treated (C, D) and sonication treated menisci (E, F). Note that images of A, C, E and B, D, F were taken at central site ×40 and at surface site ×40, respectively.

by orange line in Fig.3. High stiffness values indicate high elasticity and vice versa. (2) Relative sample compression was measured by indenter position in relation to absolute sample height. Compression is an indicator for viscosity and characterizes the ability of a sample to evade the indenter. (3) Residual force is load measured at the end of the static compression phase as shown by red tetragon in Fig. 2 and Fig. 3. The 'residual force' is influenced by the ability of tissue to evade the indenter in unconstraint compression as well as by the reset forces present in the tested tissue. High residual forces thereby indicate more elastic than viscous properties. The experiments were performed in cyclic loading to simulate physiologic stress.

E. Statistical Analysis

Comparisons between the processes were performed using Student t-test. Data were analyzed using SPSS. Bar graphs represented as means and standard deviation (SD). The significance level (p) was set at 0.05. Not significant level indicated as NS.

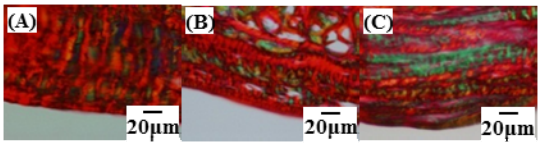

Fig.5 Photograph of picrosirius red staining of native (A: surface, ×40) immersion treated (B: surface, ×40) and sonication treated menisci (C: surface, ×40).

III. RESULTS

A. Histological Analyses of Decellularization

Representative images of EVG staining are shown in Fig. 4. The remaining nuclei were significantly decreased in sonication treatment than immersion treatment.

B. Histological Analyses of Collagens

Representative images of picrosirius red staining are shown in Fig. 5. The samples treated by sonication sustained their type-1 and type-3 collagens. There were no significant difference between three samples (A, B and C) for their collagen construct and density.

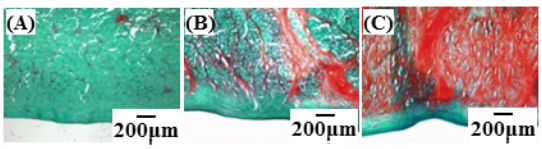

Fig.6. Photograph of picrosirius red staining of native (A), immersion treated (B) and sonication treated menisci (C). All images were taken at central surface×4.

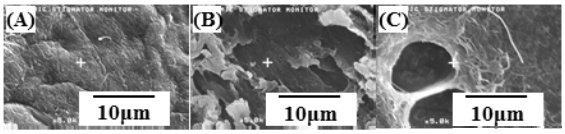

Fig. 7 Representative SEM images from native (A), immersion treated (B) and sonication treated menisci (C). Note that images of A, B and C were taken at ×5000, respectively.

C. Histological Analyses of GAG

Representative images of safranin-O/fast green staining are shown in Fig. 6. The samples treated by sonication show that GAG decreased significantly compared with untreated native and immersion treatment as shown in Fig. 6.

D. SEM observation and analysis

Representative images of SEM are observed from surface view of sonicated as shown in Fig. 7. The decellularized samples by immersion and sonication show lower density of ECM fibers which were found barely formed. The less dense fibers thus lead to development of holes.

E. Biomechanical parameters

The mean sample height was 3.08±0.23 mm. All parameters were gradually increased cycle by cycle. Stiffness and compression were increased in treated samples than native samples. Residual force was decreased in treated samples than native samples. However, there are no statistically significant between three cycles for sonicated scaffolds.

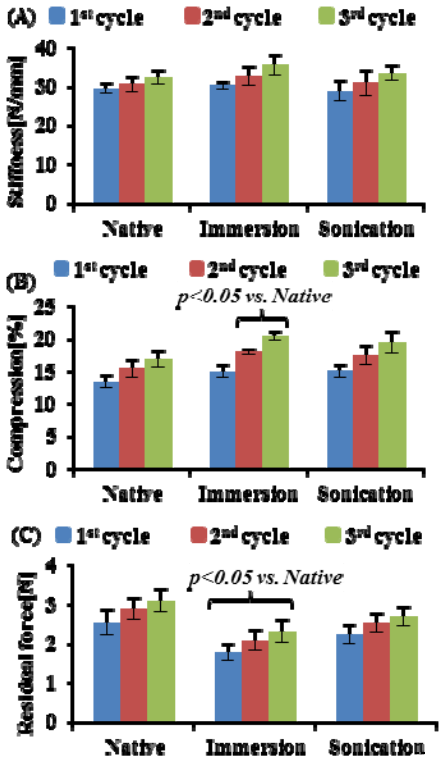

Fig. 8 Stiffness (A), compression (B), and residual force (C) were determined from native, immersion treated and sonication treated menisci. There were no significant ($p > 0.05$) differences between untreated native and sonication treated scaffolds.

IV. Discussion

Meniscus contains approximately 98% type I collagen and less than 1% of GAG contained proteoglycans [12]. Collagen forms meniscus by fibrous construction. GAG keeps fluid in meniscus. It is thought that the denatured collagen and GAG changed biomechanical properties. In the study, we demonstrated histologically and biomechanically that sonication treatment was capable to completely decellularize menisci with no significant effect on its biomechanical properties.

It shows that the immersion treatment using SDS could decellularize meniscus but decellularization rate is lower comparing with the sonication treatment (see in Fig. 4). We found that almost all of nuclei could be removed by sonication treatment. There are two speculations, which sonication is able to influence decellularization rate. First, vibration by sonication assists SDS solution to penetrate to the inside of samples. Second, sonication has its cavitation effects to destroy nuclei in the scaffolds.

The intensity of safranin-O staining is directly proportional to the proteoglycan content in normal cartilage. Safranin-O stains sulfated GAGs red and Fast Green stains collagen green. Safranin-O binds to glucosaminoglycan (GAG) an orange color and is often used to stain articular cartilage. Fast green, the contrast stain of Safranin-O, is a sulfate group containing acidic substrate, which binds strongly to the amino group on protein and thereby strongly stains non-collagen sites.

Cyclic testing was performed to simulate physiological loading conditions and to gain more information about viscoelastic behavior of the meniscus. Stiffness, compression, and residual force were measured as important parameters of viscoelasticity. The dynamic compression phase analyzed the elastic properties of the meniscus. ‘‘Stiffness’’ was measured during dynamic compression of the meniscus. For stiffness calculation, we used the linear-elastic part of the load curve. The ‘‘compression’’ of the sample is an indicator of viscosity as it characterizes the ability of the sample to expand. The ‘‘residual force’’ is important for characterization of viscoelastic behavior of material. It is influenced by the ability of the tissue to expand under unconstraint compression and by the amount of reset forces present in the tissue. Tissues with high residual forces would behave more elastic than viscous and vice versa.

GAG denaturation by sonication treatment decreases the ability of meniscus to maintain water. Considering the function of GAG’s as important load distributors, the observed changes are likely to be mediated mainly by ultrasound. Increase of stiffness throughout cyclic loading is probably caused by progressive compression of the tissue. Lower residual forces mean a decrease of the elastic properties of the tissue, since the reset forces within the tissue diminish.

We believe that the decrease of residual force after the treatment can be explained by the structural changes of the ECM due to mainly denaturation of GAG. The residual force increased throughout cyclic testing in both native and processed meniscus indicating a compaction of the ECM. SEM of the sonication treated samples showed holes. However, these holes did not affect biomechanical properties. There are no statistically significant between three cycles for tested sonicated scaffold as type-1 and type-3 collagens were maintained in sonicated samples. It is necessary to study decellularization condition without GAG denaturation for further research.

V. Conclusion

We are successful to completely decellularize bovine menisci using the sonication treatment without significantly affecting its biomechanical properties. These cell-free constructs could serve as excellent scaffolds with a preserved extracellular matrix maintaining the natural biomechanical properties.

Acknowledgment

This study was supported in part by a grant from the Ministry of Education, Culture, Sport, Science and Technology (MEXT) for its finance support through a Strategic Research Foundation Grant for Private Universities (S0801023). The authors are thankful to Prof. Masato Tanaka, Dr. Kasuaki Muramatu and Susumu Minezaki for their valuable advices.

References

[1] G Allison, et al. Performance of a sterile meniscal allograft in an ovine model. Clin Orthop Relat Res.; 467:1868–1876, 2009.

[2] E Van Arkel, et al. Survival analysis of human meniscal transplantations. J Bone Joint Surg Br; 84:227–231, 2002.

[3] V Martinek, et al. Second generation of meniscus transplantation: in-vivo study with tissue engineered meniscus replacement. Arch Orthop Trauma Surg 126:228–234, 2006.

[4] D Hutmacher, et al. An introduction to biodegradable materials for tissue engineering applications. Ann Acad Med Singapore; 30:183-191, 2001.

[5] D Schmidt, et al. Tissue engineering of heart valves using decellularized xenogeneic or polymeric starter matrices. Phil. Trans. R. Soc. B; 362:1505–1512, 2007.

[6] W Thomas, et al. Decellularization of tissues and organs. Bioma; 19:3675-83, 2006.

[7] A Azhim, et al. Decellularization of meniscal tissue using ultrasound chemical process for tissue-engineered scaffold applications. WCB, IFMBE Proceedings; 31:915–918, 2010.

[8] B. Niemczewski, et al. Chemical activation of ultrasonic cavitation. Ultrasonics Sonochemistry; 6-4:211-221, 1999.

[9] Y Wang, et al. Antitumor effect of microbubbles enhanced by low frequency ultrasound cavitation on prostate carcinoma xenografts in nude mice. Exp Ther Med; 3:187-191, 2012.

[10] P Buma, et al. Tissue engineering of the meniscus. Biomaterials; 25: 1523–1532, 2004.

[11] P Diehl, et al. Biomechanical and characterization of a human acellular meniscus scaffold. Journal of Biomedical Materials Research Part A. J Orthop Sci; 11:380–385, 2006.

[12] Y Sun,.et al. Histological examination of collagen and proteoglycan changes in osteoarthritic menisci. Open Rheumatol J.; 6:24-32, 2012.

[13] D Maier, et al. In vitro analysis of an allogenic scaffold for tissue-engineered meniscus replacement. J Orthop Res; 25:1598–1608, 2007.

[14] V Tienen et al. Tissue in growth and degradation of two biodegradable porous polymers with different porosities and pore sizes. Biomaterials; 23:1731–1738, 2002.

[15] A. Azhim, et al. The use of sonication treatment to completely decellularize blood arteries: A pilot study. Conf. Proc. IEEE Eng. Med. Biol. Soc., Boston, 2468-2471, 2011